THE ASTROPHYSICAL JOURNAL, 492:421–427, 1998 January 10

EVOLUTION OF THE PAIRWISE PECULIAR VELOCITY DISTRIBUTION FUNCTION IN LAGRANGIAN PERTURBATION THEORY

NAOKI SETO
Department of Physics, Faculty of Science, Kyoto University, Kyoto 606-01, Japan
AND
JUN'ICHI YOKOYAMA
Yukawa Institute for Theoretical Physics, Kyoto University, Kyoto 606-01, Japan
Received 1997 May 30; accepted 1997 August 21

ABSTRACT

The statistical distribution of the radial pairwise peculiar velocity of galaxies is known to have an exponential form as implied by observations and explicitly shown in N-body simulations. Here we calculate its statistical distribution function using a Lagrangian perturbation theory assuming that the primordial density fluctuations are Gaussian distributed. We show that the exponential distribution is realized as a transient phenomenon on megaparsec scales in the standard cold-dark-matter model.

Subject headings: cosmology: theory — large-scale structure of universe — methods: statistical

1. INTRODUCTION

The pairwise velocity distribution function of galaxies plays an important role in translating observed clustering properties in redshift space to those in real space. Since Peebles (1976) proposed the adoption of a distribution function of an exponential form, a number of observational analyses (Davis & Peebles 1983; Hale-Sutton et al. 1989; Fisher et al. 1994; Marzke et al. 1995) have confirmed that it provides a better fit than other distributions. The results of N-body simulations (Efstathiou et al. 1988; Veda, Itoh, & Suto 1993; Fisher et al. 1994) have shown more directly that the distribution indeed has an exponential tail with a flatter peak. More recently, Zurek et al. (1994, hereafter ZQSW) have shown that the pairwise halo velocity distribution function has a skewed exponential shape with a sharp peak in their simulations of cold-dark-matter (CDM) models with a higher resolution.

In spite of the simplicity of the shape of the function, its origin had been a mystery for a long time. It was expected that the exponential shape arose as a result of highly nonlinear gravitational effects, because linear evolution preserves the initial shape of the velocity distribution, which is usually assumed to be Gaussian.

Recently Sheth (1996) and, independently, Diaferio & Geller (1996) proposed a model that explains the exponential shape of the pairwise velocity distribution function. They considered a universe composed of isothermal clumps whose mass function is given by the Press & Schechter (1974) theory or observation. Then they assumed that the velocity distribution of galaxies in each clump is Maxwellian, whose dispersion is determined by its mass, and that each pair of galaxies of interest is contained in a common clump. They have calculated the weighted sum of the pairwise velocity distribution function and shown that it indeed has an exponential tail. Diaferio & Geller (1996) have further discussed that if they adopt a velocity distribution function of galaxies in a clump that is more highly peaked than Gaussian, they can reproduce the sharp exponential core of the final pairwise velocity distribution.

Although their idea is interesting and attractive, its applicability is limited to a highly nonlinear regime with a small separation up to $R \lesssim 1\ h^{-1}$ Mpc (Diaferio & Geller 1996), because their approach is valid only when each pair belongs to the same nearly virialized clump whose typical size is around $1\ h^{-1}$ Mpc. On the other hand, the results of N-body simulations clearly show that the exponential shape is kept for much larger separations up to $\sim 5.5\ h^{-1}$ Mpc (ZQSW) and for scales with a small value of the two-point correlation function, $\xi \sim 0.1$ (Efstathiou et al. 1988; Fisher et al. 1994). This motivates us to consider a different approach for explaining the exponential shape on these scales; that is, not only highly nonlinear effects but also semi-nonlinear dynamics may play a role in producing the exponential feature.

In the present paper we calculate the pairwise velocity distribution function in the semi-nonlinear regime using a Lagrangian perturbation theory known as the Zeldovich approximation (Zeldovich 1970), assuming that the primordial density fluctuation is random Gaussian. In this approximation, each mass element moves in a remarkably simple manner. In particular, the peculiar velocity field remains proportional to the "shift" vector, which is determined by the profile of the initial density fluctuation. Hence, starting from a Gaussian fluctuation, the statistical distribution of the one-point peculiar velocity field remains Gaussian (Kofman et al. 1994). The pairwise velocity distribution of an arbitrary fixed separation, however, is obtained by an appropriate weighted sum of the initial distribution function and can result in markedly non-Gaussian distributions in the semi-nonlinear regime. As a result, an exponential shape is observed in the course of evolution as seen below.

The rest of the paper is organized as follows. In § 2 we formulate the pairwise peculiar velocity distribution function in the Zeldovich approximation as a function of the initial relative velocity distribution, assuming that it is Gaussian. Then in § 3 we calculate it explicitly for the standard cold-dark-matter (CDM) model spectrum. We first trace its time evolution and then compare our results corresponding to the present epoch with N-body simulations done by ZQSW. Finally, § 4 is devoted to discussion and the conclusion.

2. PAIRWISE VELOCITY DISTRIBUTION IN ZELDOVICH APPROXIMATION

In the Zeldovich approximation (ZA), the Eulerian posi-

tion, $\boldsymbol{x}(t)$, of a mass element is given by a function of its Lagrangian or initial coordinate $\boldsymbol{q}$ as

$$\boldsymbol{x}(t) = \boldsymbol{q} + D(t)\boldsymbol{p}(\boldsymbol{q}) , \tag{1}$$

where $\boldsymbol{p}(\boldsymbol{q})$ is a shift vector and $D(t)$ is a growth factor. The density contrast, $\delta(\boldsymbol{x}, t)$, reads

$$\delta(\boldsymbol{x}, t) = \left| \frac{\partial(x_1, x_2, x_3)}{\partial(q_1, q_2, q_3)} \right|^{-1} - 1 \simeq -D(t)\nabla_{\boldsymbol{q}} \cdot \boldsymbol{p}(\boldsymbol{q}) , \tag{2}$$

where the latter approximate equality holds when δ is small. $D(t)$ is usually identified with the growth factor of the linear growing mode, and we do so here, too, but it can, in principle, be an arbitrary linear combination of linear growing and decaying modes. Then from equation (1) the peculiar coordinate velocity also has only the growing mode in the former case,

$$\boldsymbol{v}(t) \equiv \dot{\boldsymbol{x}}(t) = \dot{D}(t)\boldsymbol{p}(\boldsymbol{q}) , \tag{3}$$

so it should be identified with the growing longitudinal velocity.

Let us consider the time evolution of elements A and B with the Lagrangian coordinates $\boldsymbol{q}_A$ and $\boldsymbol{q}_B \equiv \boldsymbol{q}_A + \boldsymbol{r}$, respectively. The Eulerian position and peculiar velocity at each point read

$$\begin{aligned} \boldsymbol{x}_A(t) &\equiv \boldsymbol{x}(\boldsymbol{q}_A, t) = \boldsymbol{q}_A + D(t)\boldsymbol{p}(\boldsymbol{q}_A) \equiv \boldsymbol{q}_A + D(t)\boldsymbol{p}_A , \\ \boldsymbol{x}_B(t) &\equiv \boldsymbol{x}(\boldsymbol{q}_B, t) = \boldsymbol{q}_B + D(t)\boldsymbol{p}(\boldsymbol{q}_B) \equiv \boldsymbol{q}_B + D(t)\boldsymbol{p}_B , \\ \boldsymbol{v}_A(t) &\equiv \boldsymbol{v}(\boldsymbol{q}_A, t) = \dot{D}(t)\boldsymbol{p}_A , \\ \boldsymbol{v}_B(t) &\equiv \boldsymbol{v}(\boldsymbol{q}_B, t) = \dot{D}(t)\boldsymbol{p}_B . \end{aligned} \tag{4}$$

We investigate the time evolution of their relative velocity,

$$\begin{aligned} \boldsymbol{v}_{AB}(t) &\equiv \boldsymbol{v}_B(t) - \boldsymbol{v}_A(t) = \dot{D}(t)(\boldsymbol{p}_B - \boldsymbol{p}_A) \\ &\equiv \boldsymbol{v}_{\parallel}(t) + \boldsymbol{v}_{\perp}(t) , \end{aligned} \tag{5}$$

where $\boldsymbol{v}_{\parallel}(t)$ and $\boldsymbol{v}_{\perp}(t)$ represent components parallel and perpendicular to $\boldsymbol{r}_{AB}(t) \equiv \boldsymbol{x}_B(t) - \boldsymbol{x}_A(t)$. They read

$$\begin{aligned} \boldsymbol{v}_{\parallel}(t) &= \frac{\boldsymbol{v}_{AB}(t) \cdot \boldsymbol{r}_{AB}(t)}{|\boldsymbol{r}_{AB}(t)|^2} \boldsymbol{r}_{AB}(t) \equiv v_{\parallel}(t) \frac{\boldsymbol{r}_{AB}(t)}{r_{AB}(t)} , \\ \boldsymbol{v}_{\perp}(t) &= \boldsymbol{v}_{AB}(t) - \boldsymbol{v}_{\parallel}(t) , \end{aligned} \tag{6}$$

respectively, where $r_{AB}(t)$ and $v_{\parallel}(t)$ are given by

$$r_{AB}^2(t) = \left(r + \frac{D}{\dot{D}_i} v_{\parallel i} \right)^2 + \left(\frac{D}{\dot{D}_i} v_{\perp i} \right)^2 , \tag{7}$$

$$v_{\parallel}(t) = \frac{\dot{D}}{r_{AB}(t)} \left(\frac{r v_{\parallel i}}{\dot{D}_i} + \frac{D v_{ABi}^2}{\dot{D}_i^2} \right) . \tag{8}$$

Here the suffix i denotes quantities at the initial time $t = t_i$ when $D(t_i) \equiv D_i$ was negligibly small.

Thus, one can calculate the probability distribution function (PDF), $P(V; R, t)$, of the pairwise peculiar velocity $v_{\parallel}(t) = V$ with separation $r_{AB}(t) = R$ from the initial PDF, $p(v_{\parallel i}, v_{\perp xi}, v_{\perp yi}; r)$, as

$$\begin{aligned} P(V; R, t) = \frac{1}{4\pi R^2} \int & 4\pi r^2 dr\, dv_{\parallel i}\, dv_{\perp xi}\, dv_{\perp yi}\, p \\ & \times (v_{\parallel i}, v_{\perp xi}, v_{\perp yi}; r) \delta(R - r_{AB}(t)) \delta(V - v_{\parallel}(t)) . \end{aligned} \tag{9}$$

Here $v_{\perp xi}$ and $v_{\perp yi}$ are the two components of $\boldsymbol{v}_{\perp i}$ perpendicular to each other. From the global isotropy the initial PDF depends on $v_{\parallel i}$ and $v_{\perp i} \equiv \sqrt{v_{\perp xi}^2 + v_{\perp yi}^2}$ only. We find, after some manipulation,

$$P(V; R, t) = \frac{2\pi \dot{D}_i^3}{D^2 \dot{D}} \int_{r*}^{\infty} r\, dr p(v_{\parallel i}^*, v_{\perp i}^*; r) , \tag{10}$$

with

$$v_{\parallel i}^* \equiv \frac{\dot{D}_i}{D} \left[\frac{R}{r} \left(R - \frac{D}{\dot{D}} V \right) - r \right] , \tag{11}$$

$$v_{\perp i}^* \equiv \frac{\dot{D}_i}{D} R \left[1 - \frac{1}{r^2} \left(R - \frac{D}{\dot{D}} V \right)^2 \right]^{1/2} , \tag{12}$$

$$r^* \equiv \left| R - \frac{D}{\dot{D}} V \right| . \tag{13}$$

In order to evaluate the desired PDF, let us specify the initial PDF, $p(v_{\parallel i}^*, v_{\perp i}^*; r)$. Since we are dealing with only the longitudinal mode, in the initial or linear regime the peculiar velocity is related to $\delta(\boldsymbol{x}, t)$ or its Fourier transform, $\delta_{\boldsymbol{k}}(t)$, as

$$\boldsymbol{v}(\boldsymbol{x}, t_i) = i \frac{\dot{D}_i}{D_i} \int \frac{\boldsymbol{k}}{k^2} \delta_{\boldsymbol{k}}(t_i) e^{i\boldsymbol{k} \cdot \boldsymbol{x}} \frac{d^3k}{(2\pi)^{3/2}} \tag{14}$$

(Peebles 1980). Assuming the initial density fluctuation is random Gaussian with the power spectrum $P_i(k)$ defined by

$$\langle \delta_{\boldsymbol{k}}(t_i) \delta_{\boldsymbol{k}'}^*(t_i) \rangle = P_i(k)(2\pi)^3 \delta(\boldsymbol{k} - \boldsymbol{k}') , \tag{15}$$

we find the initial pairwise peculiar velocities are also Gaussian distributed with the two-point correlation functions (Górski 1988):

$$\begin{aligned} \langle v_{\parallel i} v_{\parallel i} \rangle &= \frac{8\pi}{3} \left(\frac{\dot{D}_i}{D_i} \right)^2 \int dk P_i(k) \left[1 - 3j_0(kr) + 6 \frac{j_1(kr)}{kr} \right] \\ &\equiv Q_{\parallel}(r) , \end{aligned} \tag{16}$$

$$\begin{aligned} \langle v_{\perp xi} v_{\perp xi} \rangle &= \langle v_{\perp yi} v_{\perp yi} \rangle \\ &= \frac{8\pi}{3} \left(\frac{\dot{D}_i}{D_i} \right)^2 \int dk P_i(k) \left[1 - 3 \frac{j_1(kr)}{kr} \right] \\ &\equiv Q_{\perp}(r) . \end{aligned} \tag{17}$$

One can also express $Q_{\parallel}(r)$ and $Q_{\perp}(r)$ in terms of the integral of the initial two-point correlation function, $\xi_i(r)$, as

$$Q_{\parallel}(r) = \frac{2}{3} \left(\frac{\dot{D}_i}{D_i} \right)^2 \left[J_2(r) - \frac{J_5(r)}{r^3} \right] \equiv \left(\frac{\dot{D}_i}{D_i} \right)^2 S_{\parallel}(r) , \tag{18}$$

$$Q_{\perp}(r) = \left(\frac{\dot{D}_i}{D_i} \right)^2 \left[\frac{2}{3} J_2(r) - \frac{J_3(r)}{r} + \frac{J_5(r)}{3r^3} \right] \equiv \left(\frac{\dot{D}_i}{D_i} \right)^2 S_{\perp}(r) , \tag{19}$$

where

$$J_n(r) \equiv \int_0^r \xi_i(r) r^{n-1} dr , \tag{20}$$

(Peebles 1993, § 21). We thus find

$$\begin{aligned} p(v_{\parallel i}^*, v_{\perp i}^*; r) &= \frac{e^{-W}}{\sqrt{(2\pi)^3 Q_{\parallel}(r) Q_{\perp}^2(r)}} , \\ W &\equiv \frac{(v_{\parallel i}^*)^2}{2Q_{\parallel}(r)} + \frac{(v_{\perp i}^*)^2}{2Q_{\perp}(r)} . \end{aligned} \tag{21}$$

We can therefore obtain the desired PDF, $P(V; R, t)$, through the integration in equation (10) if we specify $\xi_i(r)$ or $P_i(k)$. The final expression reads

$$P(V; R, t) = \frac{1}{\sqrt{2\pi}} \frac{D}{\dot{D}} \left(\frac{D_i}{D}\right)^3 \int_{r*}^{\infty} r\, dr\, \frac{e^{-W}}{\sqrt{S_{\parallel}(r) S_{\perp}^2(r)}}, \quad (22)$$

$$W = \frac{1}{2}\left(\frac{D_i}{D}\right)^2 \left\{ \frac{1}{S_{\parallel}(r)} \left[\frac{R}{r}\left(r - \frac{D}{\dot{D}} V\right) - r \right]^2 + \frac{R^2}{S_{\perp}(r)} \left[1 - \frac{1}{r^2}\left(r - \frac{D}{\dot{D}} V\right)^2 \right] \right\}.$$

We readily see that it is independent of $\dot{D}_i$. Therefore, we can deal without any difficulty with an extreme case in which peculiar velocity is set to be zero initially, as in ZQSW. Furthermore, since $S_{\parallel}(r)$ and $S_{\perp}(r)$ are proportional to D_i^2 in the linear regime when the initial condition is set, equation (22) is also independent of D_i.

Since $S_{\parallel}(r)$ and $S_{\perp}(r)$ approach the same value,

$$S_{\infty} \equiv \frac{8\pi}{3} \int dk\, P_i(k), \quad (23)$$

in the limit $r \to \infty$, we can find an analytic expression of $P(V; R, t)$ in the case in which r^* is much larger than the typical correlation scale as

$$P(V; R, t) \simeq \frac{1}{\sqrt{2\pi S_{\infty}}} \frac{D_i}{\dot{D}} \exp\left[-\frac{V^2}{2S_{\infty}} \left(\frac{D_i}{\dot{D}}\right)^2 \right] \equiv P_G(V; t), \quad (24)$$

independent of R. Thus, the PDF as calculated from ZA (eq. [22]) approaches Gaussian (eq. [24]) not only for a large separation, R, but also in the cases in which V or D is large. The latter cases, however, correspond to a highly nonlinear regime where the Zeldovich approximation is not reliable.

Note that $p(v_{\parallel i}^*, v_{\perp i}^*; r)$ in equation (21) has been normalized so that the velocity integral of $P(V; R, t)$ in equation (22) results in the two-point correlation function of the evolved density field, $\xi(R, t)$, as

$$\xi(R, t) = \int_{-\infty}^{\infty} P(V; R, t) dV - 1 \quad (25)$$

(Bharadwaj 1996).

3. PAIRWISE VELOCITY DISTRIBUTION IN CDM MODEL

3.1. *CDM Power Spectrum*

In this section, we calculate equation (22) with a specific model. We adopt the standard CDM model as a typical model of structure formation, which has also been employed by ZQSW; namely, consider the Einstein–de Sitter universe with the current Hubble parameter $H_0 = 50$ km s^{-1} Mpc^{-1}. We also normalize the scale factor $a = 1$ at present and set $D = a$. The initial power spectrum of density fluctuation is taken from Efstathiou, Bond, & White (1992) as

$$P_i(k) = \frac{BD_i^2\, k}{\{1 + [\alpha k + (\beta k)^{3/2} + (\gamma k)^2]^{\nu}\}^{2/\nu}}, \quad (26)$$

with $\alpha = 25.6$ Mpc, $\beta = 12$ Mpc, $\gamma = 6.8$ Mpc, and $\nu = 1.13$. B is the normalization factor that may be determined from the anisotropy of microwave background radiation as

$$B = \frac{12\Omega_0^{-1.54}}{5\pi H_0^4} \left(\frac{Q_{\rm rms}}{T_0}\right)^2, \quad (27)$$

where $Q_{\rm rms}$ is the quadrupole fluctuation amplitude and $T_0 = 2.73$ K is the current temperature. The 4 yr COBE data give $Q_{\rm rms-PS} \simeq 15.3$ μK (Górski et al. 1996), while the value ranges between $Q_{\rm rms} = 9.5$ μK and 23.2 μK in the simulations of ZQSW.

3.2. *Typical Time Evolution*

First, we show how the distribution function of a fixed comoving separation, R, evolves in time. Figure 1*a* depicts the evolution of $P(V; R, t)$ for the comoving scale corresponding to $R = 2$ Mpc today at $D = 0.05$, 0.1, 0.2, 0.5, 1.0, and 10.0. The horizontal velocity axis is normalized by the one-point velocity dispersion proportional to $D\dot{D}$, and the numbers on the velocity axis apply for $D = 1$ only. Figure 1*b* represents time evolution for the comoving scale $R = 6$ Mpc today. These two figures imply that the negative tail develops much faster than the positive part from symmetric Gaussian distribution, properly reflecting the attractive nature of gravitational interaction. In the intermediate stage of the evolution around $D = 0.5$–1 for Figure 1*a* and $D \sim 1$ for Figure 1*b*, an exponential shape is prominent around the peak. We thus find that the exponential pairwise peculiar velocity distribution can be realized as a result of semi-nonlinear dynamics of the Lagrangian perturbation theory.

In ZA, however, each mass element moves kinematically (eq. [1]) even after shell crossing; hence, structures or correlations are destroyed as we extrapolate the evolution with it. As is seen in Figure 1, the distribution becomes practically Gaussian again by the epoch $D = 10$, except around $V = 0$. In this highly nonlinear regime, ZA is by no means valid. We thus see that non-Gaussian shape of the distribution function $P(V; R, t)$ with a nearly exponential form near the peak is realized in this approximation as a transient phenomenon in the semi-nonlinear regime.

Finally, we briefly comment on the evolution of the two-point correlation function of the density field $\xi(R; t)$ obtained from equation (25). On the comoving $R = 6$ Mpc scale, it evolves from 0 to 0 with the maximum value of 1.0 at $D = 1.2$. ZA predicts a smaller amplitude of $\xi(R; t)$ than N-body simulations in the nonlinear regime (Schneider & Bartelmann 1995; Weiss, Gottlober, & Buchert 1996). We return to this point below.

3.3. *Dependence on the Separation*

Next, we set $D = 1$ and analyze dependence on the separation R. We plot the new distribution function for the CDM spectrum normalized by COBE data, $Q_{\rm rms} = 15.3$ μK, in Figure 2*a* on scales of $R = 2$, 6, and 10 Mpc. In Figure 2*b* the radial velocity distribution given by the linear theory is depicted for comparison. Even at the distance of 10 Mpc, these two distributions are significantly different from each other.

As mentioned in the last subsection, with the original CDM power spectrum ZA predicts a smaller magnitude of the correlation function in the nonlinear regime as a result of the fact that mass elements continue streaming even after shell crossing without getting bounded and virialized. To cure this problem, it has been suggested in the literature

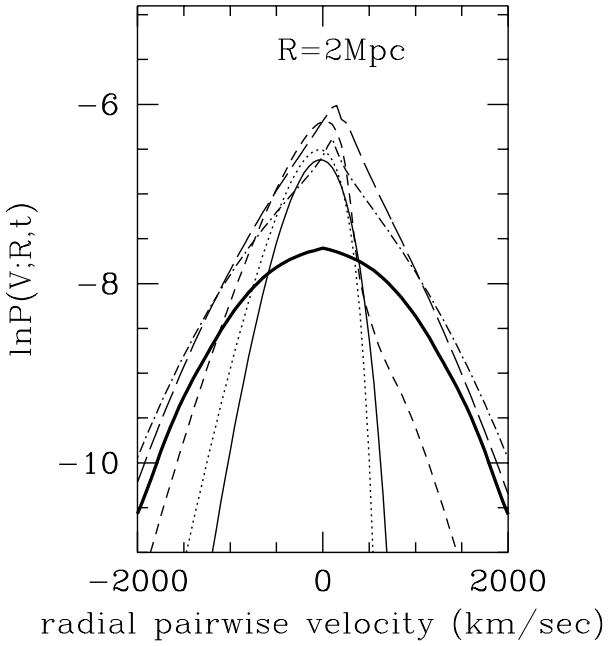

FIG. 1*a*

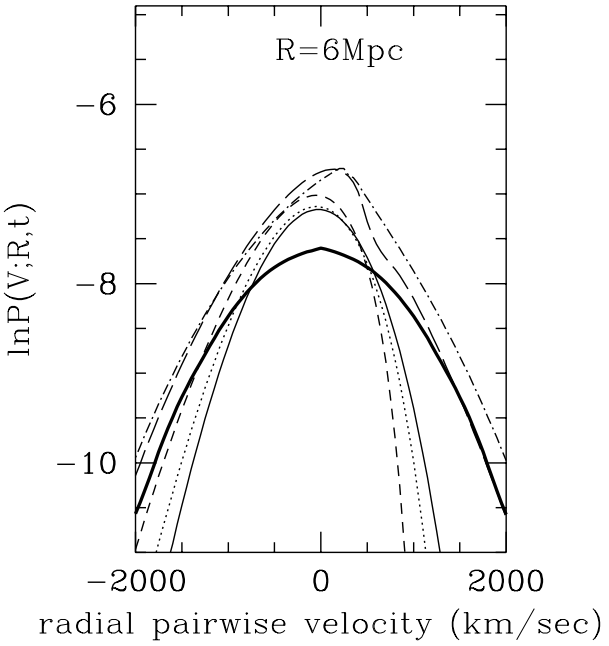

FIG. 1*b*

FIG. 1.—Evolution of the radial pairwise velocity distribution $P(V; R, t)$ for the comoving separations (*a*) $R = 2$ Mpc and (*b*) $R = 6$ Mpc in terms of ZA with the CDM initial power spectrum with $Q_{\rm rms} = 15.3$ μK. Solid line represents the distribution at $D = 0.05$, dotted line at $D = 0.1$, short-dashed line at $D = 0.2$, long-dashed line at $D = 0.5$, dash-dotted line at $D = 1$ (corresponding to the present epoch), and thick solid line at $D = 10.0$. To compare the statistical shape at different epochs, the velocity axis has been normalized by the one-point velocity dispersion proportional to $D\dot{D}$, and the numbers on the velocity axis apply for $D = 1$ only.

(Coles, Mellot, & Shandarin 1993; see also Kofman et al. 1992) that the "truncated" Zeldovich approximation (TZA) be adopted, in which small-scale power of the initial density fluctuation is phenomenologically suppressed using an appropriate window function such as a Gaussian filter and then ZA is applied to the processed power spectrum,

$$P_t(k) = \exp\,(-k^2 R_f^2) P_i(k)\,, \tag{28}$$

where R_f is the filtering length determined so that the results agree with the predictions of N-body simulations. Here we choose the filtering scale $R_f = 2.2$ Mpc so that the amplitude of the two-point correlation function at $R = 6$ Mpc becomes equal to that of the simulation (ZQSW). Figure 2*c* is the distribution function based on TZA, where we find the velocity dispersion to be too small. The filtering length we have adopted here is a modest one. In fact, for the purpose of optimizing the overall performance of ZA in reproducing the clustering properties of CDM N-body simulations, an even larger value, $R_f = 5.5$ Mpc, has been suggested by Schneider & Bartelmann (1995). Then the magnitude of velocity dispersion would be even smaller. We thus find that TZA mimics properties of the actual matter distribution; however, it does so by suppressing the velocity field, and so it is not appropriate to analyze pairwise velocity field with this approximation.

Next, we compare our results with the numerical results of ZQSW, who plotted frequency distributions of pairwise velocity for the pairs with separations of 1–2 Mpc, 5–6 Mpc, and 10–11 Mpc with the same condition as the figures of ZQSW with $Q_{\rm rms} = 9.5$ μK. In Figure 3*a* we plot our result for $R = 1$ Mpc (*dotted line*) and 2 Mpc (*solid line*), as well as the Gaussian tail distribution function (*short-dashed line*), $P_G(V; t)$, defined in equation (24). Also depicted there is a long-dashed line that mimics the histogram of ZQSW near the peak where an exponential (i.e., linear in the figures) fit is good. This line has been drawn from eye fitting of Figure 7*a* of ZQSW. Similarly, in Figures 3*b* and 3*c* results for $R = 5$ and 6 Mpc and $R = 10$ and 11 Mpc are depicted together with approximate curves inferred from the N-body experiment of ZQSW.

As is seen there, we observe a systematic deviation to the right in all three scales. This is because gravitational infall is not completely taken into account in ZA. In fact, the average infall velocities calculated by ZQSW are $\langle V_{\rm num}\rangle = -280$ km s^{-1}, -355 km s^{-1}, and -276 km s^{-1} for the pairs with $R = 1$–2 Mpc, 5–6 Mpc, and 10–11 Mpc, respectively, while ZA gives $\langle V_{\rm ZA}\rangle = 14$ km s^{-1}, -0.49 km s^{-1}, and -69 km s^{-1} for $R = 2$, 6, and 11 Mpc, respectively. If we correct this deviation of average infall by shifting the origin of the velocity axis by an appropriate amount, we find that the distribution function calculated with ZA reproduces the results of numerical simulation well, especially near the peak in Figures 3*b* and 3*c*.

This means that even if ZA fails to reproduce the average infall, it predicts pairwise velocity dispersion, $\sigma_V(R)$, fairly close to the corresponding numerical values. For a symmetric exponential distribution, the velocity dispersion appears in the PDF as

$$P(V; R)dV \propto \exp\left[-\frac{\sqrt{2}\,|V|}{\sigma_V(R)}\right]dV\,. \tag{29}$$

Since the PDF obtained from N-body simulations is asymmetric, it would be more appropriate to treat the left- and right-hand sides of the peak separately. Applying the fitting function of the type of equation (29) independently on each side of the peak in Figures 3*a*–3*c*, we estimate the velocity

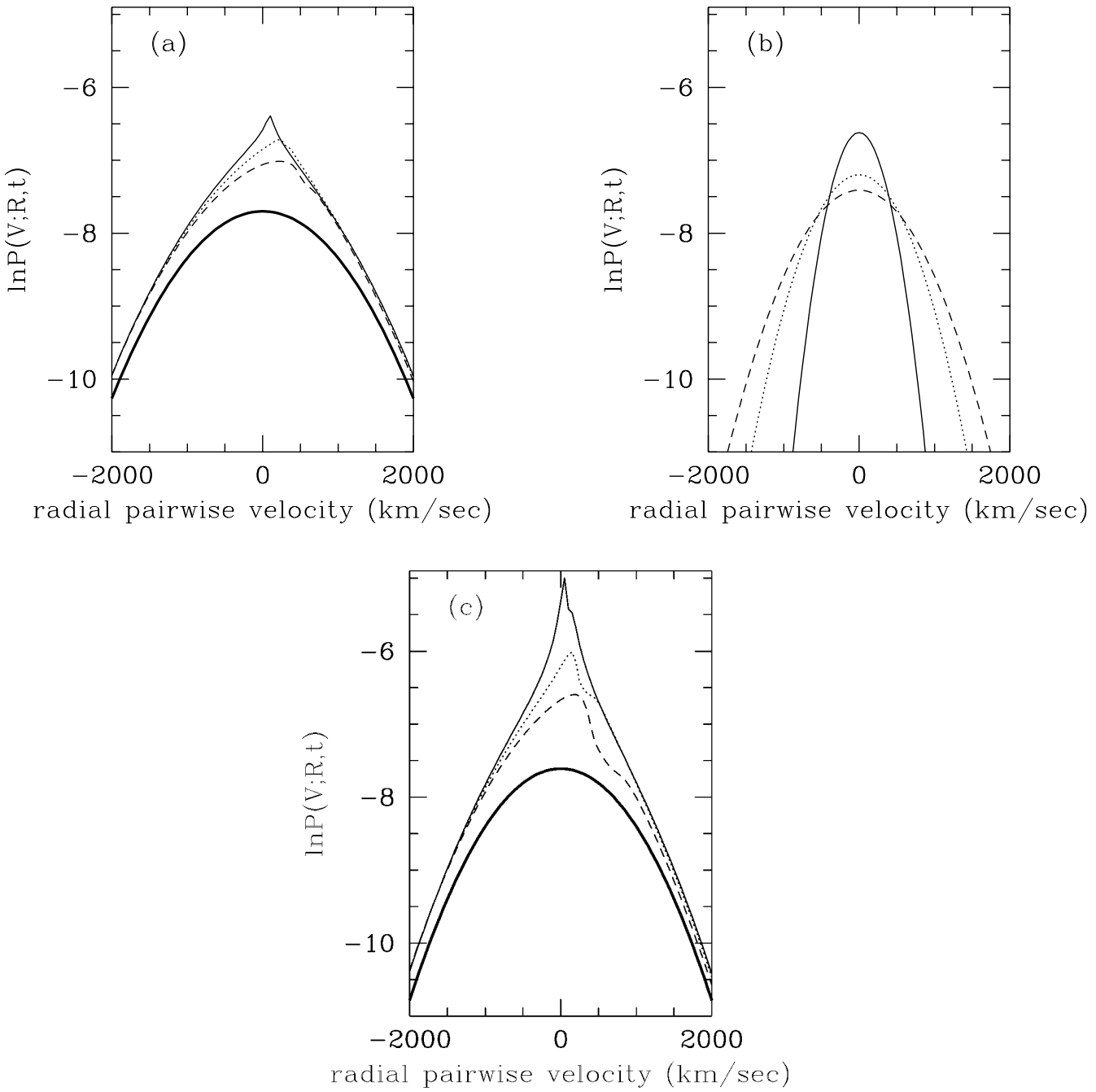

FIG. 2.—The distribution of radial pairwise distribution $P(R; V, t)$ for the separations $R = 2$ Mpc (*thin solid line*), $R = 6$ Mpc (*dotted line*), $R = 10$ Mpc (*dashed line*), and $R = +\infty$ (*thick solid line*) at present, $D = 1$. (*a*) represents the results based on ZA with the full CDM spectrum with $Q_{\rm rms} = 15.3$ μK, (*b*) is based on the linear theory with the same spectrum, (*c*) is obtained from ZA but with the truncated CDM power spectrum with the filtering length $R_f = 2.2$ Mpc.

dispersion on each side, $\sigma_{V\text{left, }right}(R)$, from the slope of each long-dashed line, which is shown in the third column of Table 1 (Figure). Also shown there are the results based on ZA. The fourth column (ZA2) is obtained from the least-squares fit between the theoretical curve (eq. [22]) and equation (29) in the region $P(V; R) < e^{-2}$ max $P(V; R)$, where the two sides are again treated independently. The fifth column (ZA1.5) is the same as ZA2 except for the narrower fitting region, $P(V; R) < e^{-1.5}$ max $P(V; R)$. In both cases the central, flatter region has been removed from fitting for $R = 11$ Mpc, just as we have done so in drawing long-dashed curves in Figure 3*c*.

As is seen there, ZA reproduces the asymmetric feature of the slope on both sides qualitatively well, and on larger scales the agreement is even quantitative.

4. DISCUSSION

In the present paper we have formulated the pairwise peculiar velocity PDF with ZA starting from Gaussian fluctuations. Using the standard CDM power spectrum, we have calculated the PDF on various scales at different epochs. As a result, we have found that even if the one-point velocity distribution remains Gaussian, a prominent non-Gaussian feature develops in the pairwise peculiar velocity

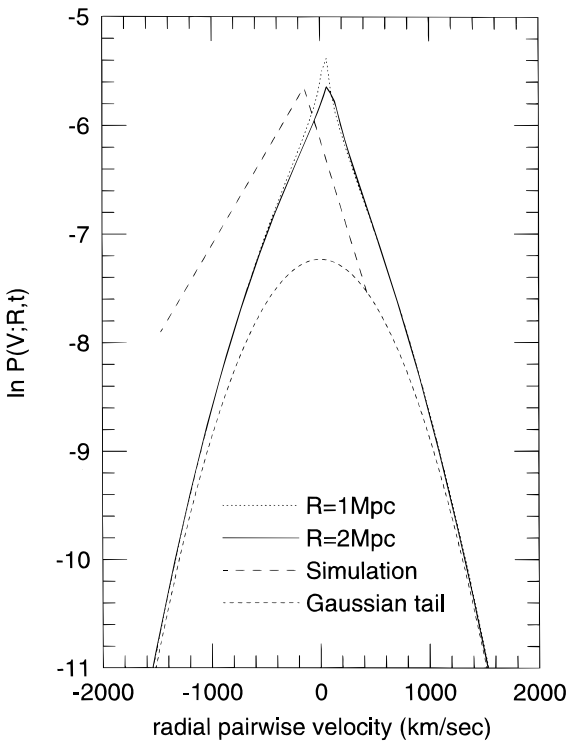

FIG. 3*a*

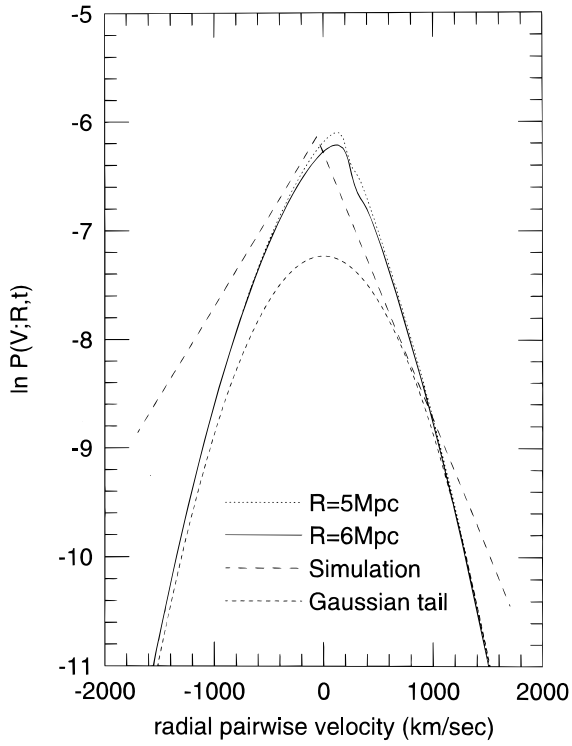

FIG. 3*b*

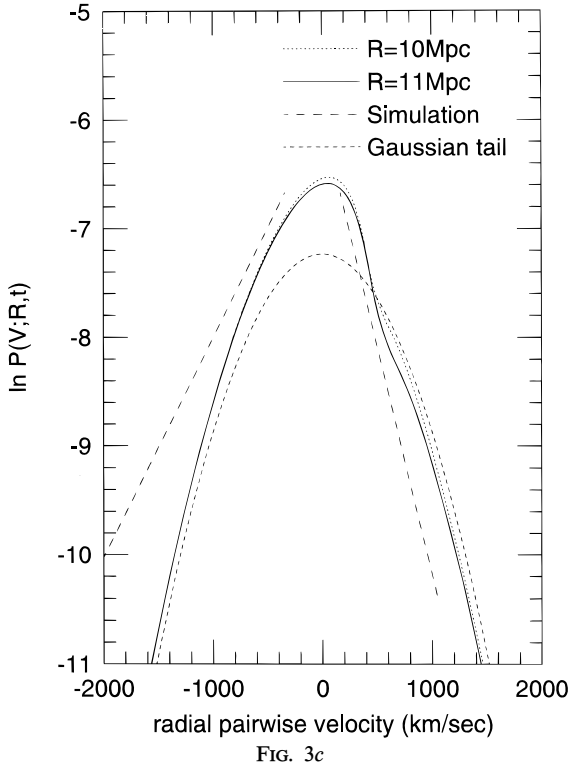

FIG. 3*c*

FIG. 3.—Schematic comparison of our formula with the results of N-body simulation of ZQSW for three typical separations at $D = 1$ with $Q_{\rm rms} = 9.5\ \mu$K. In each figure, solid and dotted lines are the PDF obtained from ZA. The long-dashed line mimics the result of ZQSW in the regions an exponential fit is reasonable. (*a*) is for the pairs for the separations $R = 1$–2 Mpc, (*b*) $R = 5$–6 Mpc, and (*c*) $R = 10$–11 Mpc. The short-dashed line is the Gaussian distribution $P_G(V; t)$ defined in eq. (24).

PDF, and we find an exponential shape on megaparsec scales before and around the epochs corresponding to the present.

One may be tempted to calculate the relative velocity PDF of pairs of higher density regions or density peaks because the numerical data of ZQSW are those of halos where galaxies are likely formed. In ZA the density contrast is a function of $\partial p_i/\partial q_j$, while the velocity field is that of p_i, and since they have no correlations in the isotropic Gaussian distribution, velocity PDF is independent of the configuration of the density field.

Previous explanations of the exponential PDF (Sheth

TABLE 1

VELOCITY DISPERSION OBTAINED FROM THE SLOPE OF THE EXPONENTIAL FITTING FUNCTION

R (Mpc)	Side	Figure[a] (10^2 km s^{-1})	ZA2[b] (10^2 km s^{-1})	ZA1.5[c] (10^2 km s^{-1})
2.....	Left	8.3	5.7	5.9
2.....	Right	4.3	4.5	4.5
6.....	Left	8.5	7.0	8.1
6.....	Right	4.2	5.1	5.5
11.....	Left	7.0	7.0	8.2
11.....	Right	3.4	4.1	3.5

[a] Based on the long-dashed lines in Figs. 3*a*–3*c*.

[b] From the least-squares fit between the theoretical curve (eq. [22]) and eq. (29) in the region $P(V; R) < e^{-2}$ max $P(V; R)$.

[c] Same as ZA2 but with a narrower fitting region, $P(V; R) < e^{-1.5}$ max $P(V; R)$.

1996; Diaferio & Geller 1996) are based on highly nonlinear dynamics of galactic systems. That is, the exponential feature appears as a result of superposition of Gaussian velocity distributions in clumps with various velocity dispersions. Hence, although this model is suitable to account for a symmetric exponential distribution with vanishing mean net relative velocity, a more elaborate treatment is necessary in order to reproduce an asymmetric exponential distribution with its peak at a negative relative velocity, as observed in numerical simulations.

The PDF based on ZA naturally realizes an asymmetric exponential feature, although it also failed to predict the location of the peak correctly at $D = 1$. In fact, as discussed in the literature (Coles et al. 1993; Schneider & Bartelmann 1995; Weiss et al. 1996), ZA does not successfully reproduce clustering properties of the density field in the regime $D \simeq 1$, and it has been suggested that the truncated spectrum be used to make the agreement better for $D \gtrsim 0.2$ (Schneider & Bartelmann 1995). On the other hand, as we have shown in Figure 2*c*, this TZA predicts too small amplitudes of the velocity dispersion. Thus, neither the original ZA nor TZA reproduces both density distribution and pairwise velocity distribution simultaneously for the present universe. Hence, it is not very certain to what extent the semi-nonlinear dynamics discussed here plays a role in realizing the actual exponential distribution in the present universe. In order to draw a more quantitative conclusion, it is desirable to compare our formula (eq. [22]) with the time evolution of N-body simulations of a CDM model, especially around the epoch $D \simeq 0.2$ up to when the original ZA suffices for reproducing the power spectrum of the density field. Unfortunately, we have been unable to do so because of the lack of published data with sufficient information about initial conditions, epoch, and separation in physical units.

Our conclusion is therefore limited to a qualitative one. Nonetheless, we believe it is worth pointing out that simple kinematics as ZA results in an exponential shape of the pairwise peculiar velocity distribution. Indeed, the pairwise PDF, which contains much more information on clustering in that its integral gives the two-point correlation function, is totally different from the one-point PDF.

We are grateful to Professor W. H. Zurek for correspondence and to Dr. Paul Haines for helpful comments. N. S. would like to thank Professor N. Sugiyama for useful comments and Professor H. Sato for his continuous encouragements. He also acknowledges support from JSPS. This work was partially supported by the Japanese Grant-in-Aid for Science Research Fund of the Ministry of Education, Science, Sports and Culture 3161 (N. S.) and 09740334 (J. Y.).

REFERENCES

Bharadwaj, S. 1996, ApJ, 472, 1
Coles, P., Mellot, A. L., & Shandarin, S. F. 1993, MNRAS, 260, 760
Davis, M., & Peebles, P. J. E. 1983, ApJ, 267, 465
Diaferio, A., & Geller, M. 1996, ApJ, 467, 19
Efstathiou, G., Bond, J. R., & White, S. D. M. 1992, MNRAS, 258, 1
Efstathiou, G., Frenk, C. S., White, S. D. M., & Davis, M. 1988, MNRAS, 235, 715
Fisher, K. B., Davis, M., Strauss, M. A., Yahil, A., & Huchra, J. P. 1994, MNRAS, 267, 927
Górski, K. 1988, ApJ, 332, L7
Górski, K., et al. 1996, ApJ, 464, L11
Hale-Sutton, D., Fong, R., Metcalfe, N., & Shanks, T. 1989, MNRAS, 237, 569
Kofman, L., Bertschinger, E., Gelb, J. M., Nusser, A., & Dekel, A. 1994, ApJ, 420, 44
Kofman, L., Pogosyan, D., Shandarin, S. F., & Melott, A. L. 1992, ApJ, 393, 437
Marzke, R. O., Geller, M. J., da Costa, L. N., & Huchra, J. P. 1995, AJ, 110, 477
Peebles, P. J. E. 1976, Ap&SS, 45, 3
———. 1980, The Large Scale Structure of the Universe (Princeton: Princeton Univ. Press)
———. 1993, Principles of Physical Cosmology (Princeton: Princeton Univ. Press)
Press, W., & Schechter, P. 1974, ApJ, 187, 425
Schneider, P., & Bartelmann, M. 1995, MNRAS, 273, 475
Sheth, R. K. 1996, MNRAS, 279, 1311
Veda, H., Itoh, M., & Suto, Y. 1993, ApJ, 408, 3
Weiss, A. G., Gottlober, S., & Buchert, T. 1996, MNRAS, 278, 953
Zeldovich, Ya. B. 1970, A&A, 5, 84
Zurek, W. H., Quinn, P. J., Salmon, J. K., & Warren, M. S. 1994, ApJ, 431, 559 (ZQSW)